THE ASTROPHYSICAL JOURNAL, 488:872–880, 1997 October 20

POINT SOURCES OF GeV GAMMA RAYS

R. C. LAMB[1] AND D. J. MACOMB[2,3]
Received 1997 March 6; accepted 1997 June 5

ABSTRACT

A catalog of γ-ray sources based on photons with energies greater than 1 GeV has been developed from observations taken by the EGRET instrument of the *Compton Gamma Ray Observatory*. The data are taken from the 4.5 yr of observation available in the public data archives. We emphasize sources that are detected using the entire database, without regard to any possible transient or variable behavior. Ten of the 57 sources reported here have not previously been reported in the catalogs developed using photons above 100 MeV in energy. Twenty-seven sources have identifications with objects seen at other wavelengths: the Large Magellanic Cloud, five pulsars, and 21 blazars. The remaining 30 sources are classified as unidentified; however, seven may be associated with Galactic supernova remnants and one source may be a Galactic X-ray binary (LSI 61 303). The 30 unidentified sources are distributed nearly uniformly along the Galactic plane and are symmetric about it. Only one of the unidentified sources has a Galactic latitude in excess of 30°, whereas, if the sources were distributed uniformly, ~ 12 would be expected on the basis of the combined EGRET exposure. A scatter plot of the flux from the unidentified sources versus Galactic latitude reveals two rather distinct categories of source: "bright" sources with fluxes greater than or equal to 4.0×10^{-8} photons cm^{-2} s^{-1} and "dim" sources with fluxes of less than 4.0×10^{-8} photons cm^{-2} s^{-1}. The absence of high-latitude bright sources is striking. The bright unidentified sources have an average Galactic latitude of 2°.7, which is consistent with a Population I distribution at distances of 1–5 kpc. The dim unidentified sources have a broader latitude distribution with an average $|b| = 13°.8$, indicating that if they are at the same average distance from the Galactic plane as the bright sources, they are paradoxically approximately 5 times closer than the bright objects on average and therefore roughly 2 orders of magnitude less luminous.

Subject headings: catalogs — gamma rays: observations — Magellanic Clouds — pulsars: general

1. INTRODUCTION

The EGRET instrument on the *Compton Gamma Ray Observatory* has surveyed the sky several times over since observations began in 1991 April. The second EGRET catalog (Thompson et al. 1995), based on data from phases 1 and 2 (1991 April–1993 November) lists 129 sources with photon energies above 100 MeV. These sources include solar flares, pulsars, γ-ray bursts, the Large Magellanic Cloud, active galaxies, and 71 sources with no firm identification. A supplement to the second catalog, incorporating observations through phase 3 (1994 October), has now been published, listing an additional 28 sources (Thompson et al. 1995). Sources with regions of the sky away from the Galactic plane ($|b| > 10°$) are discussed in a series of papers (Dingus et al. 1996; Nolan et al. 1996; Sreekumar et al. 1996; Lin et al. 1996). The four sources presented by Dingus et al. (1996) not previously reported in the EGRET catalogs bring the total number of EGRET γ-ray sources above 100 MeV to 161.

In this paper we develop a list of sources using only photons with energies above 1 GeV. The data that incorporate approximately the first 4.5 yr of observations, until the end of cycle 4 operation (through 1995 September), are taken from the EGRET public archives. We concentrate on sources that are detected using the entire composite database. Transient sources that are not significantly detected using the entire 4.5 yr of data are not discussed.

There are a number of reasons why it is useful to develop such a listing. In the first place, it is possible that a population of relatively hard, Galactic γ-ray point sources buried in the diffuse Galactic background radiation at 100 MeV may become visible at higher energies. The spectrum of the diffuse Galactic emission as modeled (Bertsch et al. 1993) falls with energy as $E^{-2.7}$ in the photon energy range of several GeV, whereas many of the already known Galactic point sources (both the identified pulsars and the unidentified sources) have spectra that are hard, with spectral indices from -1.5 to -2.2. Studies of 1 GeV γ-ray sources may eventually contribute to a better understanding of the contribution of pointlike sources to the overall Galactic emission.

In addition, at 1 GeV the angular resolution of EGRET is approximately 3.4 times better than at 100 MeV (Thompson et al. 1993). Therefore in regions of the sky where several γ-ray sources contribute, source confusion will be diminished. Of course, if one's prime objective is source detection, then the loss in photon statistics is severe (a factor of 10 for a source with a differential spectral index of -2.0); however, this may be compensated for to a large extent by the improved angular resolution and diminished background. This is borne out by a comparison of the most significant multi-GeV sources from the catalog presented here with their 100 MeV detections. There is little loss in statistical significance on average, with a few cases of even greater significance at the higher energies. Furthermore, some of the source location error regions are better defined than at lower energies, particularly for sources near the

[1] Space Radiation Laboratory, California Institute of Technology, Pasadena, CA 91125.
[2] NASA GSFC Science Support Center, NASA Goddard Space Flight Center, Greenbelt, MD 20771.
[3] Astronomy Programs, Universities Space Research Association.

Galactic plane, where the Galactic diffuse background is less at the higher energies. For such cases the smaller error regions should aid in the eventual identification of these sources with objects seen at other wavelengths. There is, however, a statistical penalty to be paid in searching the sky, since the smaller "beam size" at 1 GeV results in more effective trials.

A multi-GeV source list will be useful to the atmospheric Cerenkov detector community. Currently, such detectors are limited to photon energies above ~ 200 GeV, but there are proposals (Weekes 1996; Ong et al. 1996; Québert et al. 1996) to develop detectors to reach perhaps an order of magnitude lower in energy, substantially reducing the gap that currently exists between the energy ranges covered by space-borne pair production telescopes and by the Cerenkov technique. Since the atmospheric Cerenkov technique is a pointed technique, no sensitive all-sky survey has yet been accomplished at the energies covered by it. Thus a catalog developed from EGRET's highest energy photons will provide a useful guide for source observations with the higher energy ground-based detectors.

In the following section the methods used to derive the source list are described. Section 3 presents the detected sources. In § 4 the 26 identified sources are briefly discussed. All of the identified sources had been previously identified using lower energy EGRET photons. In § 5, the unidentified sources are discussed. From their Galactic longitude and latitude distributions, most, if not all, of the unidentified sources may be inferred to be Galactic. It will be argued that a division of these sources into two populations is reasonable. One population is composed of low-latitude, bright sources; the other is a relatively dim, possibly nearby component. Possible identifications of these categories will be discussed.

2. OBSERVATIONS AND ANALYSIS

The EGRET instrument has been well documented (Kanbach et al. 1988; Thompson et al. 1993). The ability to image photons from 30 MeV to around 10 GeV with a large collection area, coupled with the long lifetime of *CGRO*, has made EGRET the most successful pair-production telescope yet flown. At energies above 1 GeV, EGRET still has a large effective area (greater than 1000 cm^2) and field of view (appreciable sensitivity out to 30° from the instrument axis). These characteristics make EGRET as good a survey instrument above 1 GeV as it is at 100 MeV, with the caveat that most sources are much weaker above 1 GeV.

The basic database for this study is all-sky maps in both J2000 and Galactic coordinates that contain 4.5 yr of co-added data. Exposure maps and count maps for energies greater than 1 GeV for the 167 individual *CGRO* pointings that comprise the EGRET observations through phase 4 have been combined into rectangular maps with a 0°.5 $\times$ 0°.5 binning. This is the same binning used in the 100 MeV catalogs. The EGRET point-spread function (PSF) is much smaller at 1 GeV, however. The effect of this was tested by the use of smaller binnings (down to 0°.1 $\times$ 0°.1) for a limited number of viewing periods for sources in the Galactic anticenter region. The smaller binning did not result in a significant difference in estimates of detected source parameters, therefore we consider the larger binning to be acceptable. The complete database as well as the software to combine and analyze the maps are all available through the services of the *CGRO* Science Support Center.

The co-added maps were analyzed using the maximum likelihood technique (Mattox et al. 1996a). No prior knowledge about known sources was assumed. Specifically, we did not use the 100 MeV catalog as a starting point. Our source list was produced through an iterative technique of identifying significant features in likelihood maps, adding these sources to the source listing, and repeating this with the known sources being subtracted out. This process began with the Galactic map, with the celestial map being used as an alternative for high-latitude sources.

Simulations of all-sky maps have been performed in order to assess source significance. Eight maps, four each in J2000 and Galactic coordinates, were created using the actual exposure maps and the EGRET diffuse background model. The mean number of counts in each map was normalized to the total number in our database ($\sim$90,000 photons). Poisson deviations to the expected number in each bin, based on the background model smoothed with the EGRET PSF, form the simulated data. As described in Mattox et al. (1996a), the parameter used to distinguish sources from the background is the square root of the maximum likelihood test statistic. This quantity is not truly Gaussian distributed; however, as a shorthand we will use language as if it were. For example, 5 σ corresponds to a value of the square root of the maximum likelihood test statistic equal to 5. A 5 σ detection threshold provides a criterion whereby there is little doubt as to the reality of a source. As Figure 1 shows, at a 4.0 σ level, several spurious sources are expected. This plot shows the distribution of the square root of the maximum likelihood test statistic for the eight simulations along with the actual data. The plots are for the values within each 0°.5 $\times$ 0°.5 bin, so there is some "oversampling" of sources in that a source overlaps more than one bin. This oversampling is roughly a factor of 2 for the simulated maps at high values of the test statistic. The actual number of spurious sources found above 4.0 σ for the eight simulated maps was 20, with none of the spurious sources going above 4.5 σ. Given that our actual data set comprises two maps, we expect no spurious sources above 4.5 σ and 5 $\pm$ 1.2 above 4.0 σ.

With this in mind, we separate our catalog into three tables. The first represents sources with a 5 σ or greater significance. These are high-confidence sources. The second

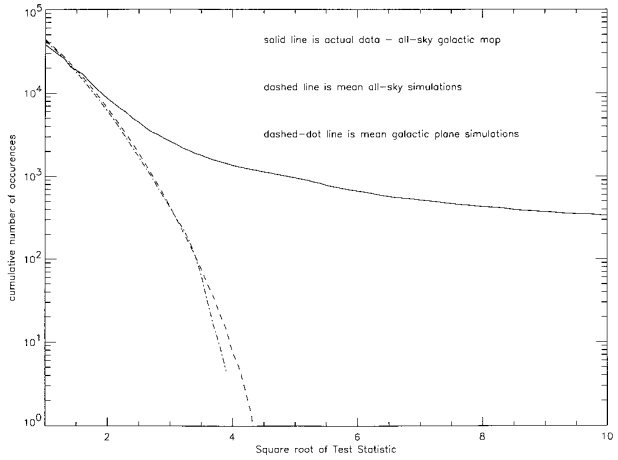

FIG. 1.—Simulations of the 1 GeV sky vs. actual data. The vertical scale gives the cumulative number of occurrences above a given σ threshold.

are sources that have significance between 4.5 and 5 σ. The majority of these low-significance sources are true γ-ray sources, and we expect at most one spurious source. We did not find any significant differences between Galactic plane simulations and high–Galactic-latitude simulations, which would have led us to treat these two regions differently, as shown in Figure 1, so we have not made a distinction based on Galactic latitude. However, the high-significance versus low-significance distinctions should provide some safety from systematic effects involving the diffuse model or other systematic errors. The final category of sources consists of those between 4.0 and 4.5 σ, which are spatially coincident with previously cataloged 100 MeV sources. These are predominantly real sources, since we detected 18 in this interval of significance; statistical fluctuations alone should produce only 5 ± 1.2. Five of these 18 sources are associated with previously catalogued 100 MeV sources and are therefore regarded as real. Any features below 4 σ are ignored for this analysis. Many such features down to 3.0 σ have been included, however, as possible sources for the likelihood analysis.

Both the likelihood analysis and simulations rely on standard software and data products, with one exception. The EGRET PSF used is not that which was found using the preflight calibration data. Instead, we have utilized an in-flight PSF based upon the count distribution of the Vela pulsar, which provided a strong steady source. This change was made because the preflight PSF did not provide a decent fit to many of the strong 1 GeV sources. The actual PSF used was arrived at iteratively, by modeling the Vela pulsar source counts as a new PSF. The main difference is that the in-flight PSF is somewhat broader. (Note: in the standard EGRET 100 MeV analysis, the database is restricted to photons that make an angle of less than 30° with respect to the spark chamber. For our 1 GeV analysis, we made no such restriction.)

The combined exposure of the 4.5 yr of data is shown in Galactic coordinates in a map in Figure 2. Regions of the highest exposure (greater than 1.8×10^9 cm^2 s) occur in the Galactic center and anticenter regions as well as in the Virgo region. The least exposed region ($\sim 2.5 \times 10^8$ cm^2 s) occurs in the region between Virgo and the Galactic anticenter region.

3. GeV SOURCE LISTS

Tables 1 and 2 give the 46 high- and six low-significance source listings, ordered by Galactic longitude. Table 3 lists the five subthreshold sources which are consistent in position with a 100 MeV source. Figure 3 plots the sources from all three tables. Both Galactic plane and high-latitude sources are well represented.

In each of Tables 1–3 the source coordinates are determined by using the location of the largest value of the maximum likelihood test statistic. The position error for a source gives the radius of the 95% confidence circle (in arcminutes), if a single number is given. If three numbers are given, they refer to a 95% confidence ellipse with semimajor and semiminor axes (in arcminutes) and orientation (in

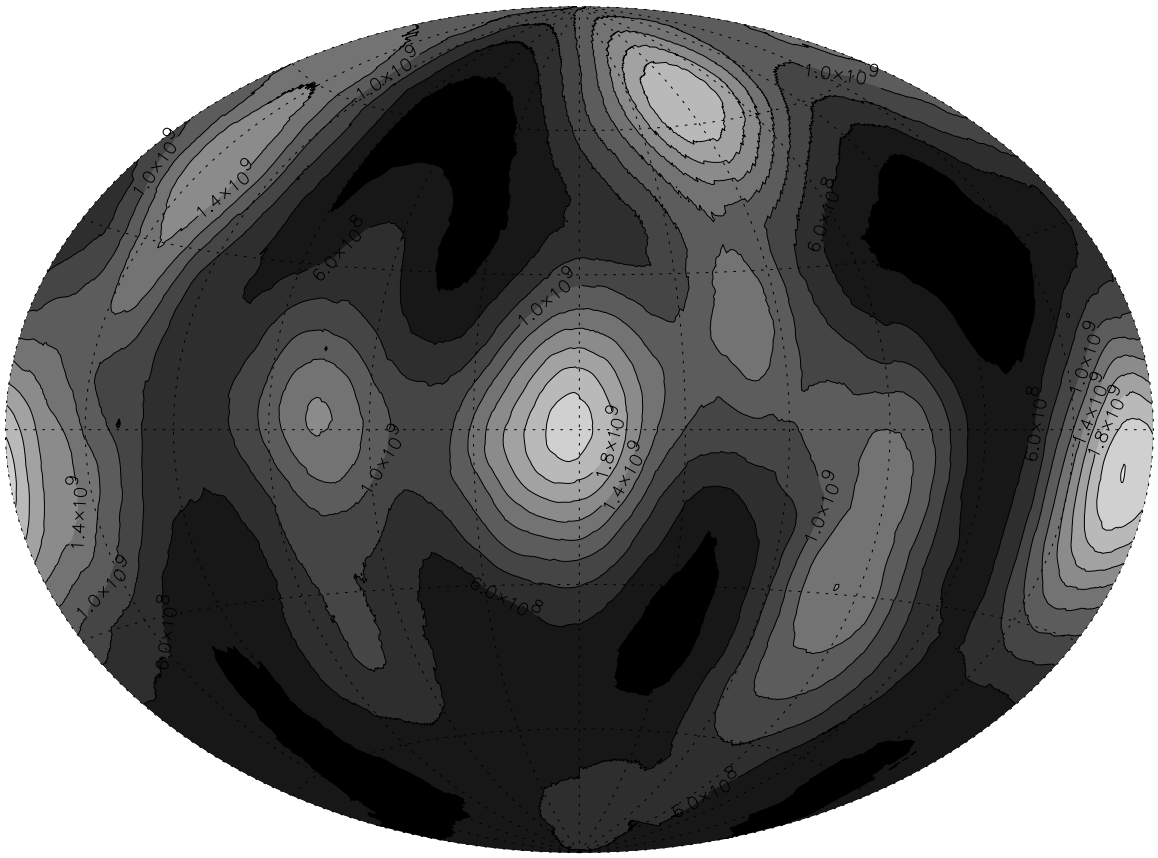

FIG. 2.—Total exposure map in units of cm^2 s. Regions of the highest exposure (greater than 1.8×10^9 cm^2 s) occur in the Galactic center and anticenter regions as well as in the Virgo region. The least exposure ($\sim 2.5 \times 10^8$ cm^2 s) occurs between Virgo and the Galactic anticenter regions.

TABLE 1

HIGH-SIGNIFICANCE SOURCES[a]

Source Name	Galactic Coordinates	Positional Error	σ	Flux	Photons	Identification
GEV J1746−2854.....	0.08, −0.08	9.6, 7.4 (8.3)	15.7	23.5 ± 1.9	489 ± 39	2EG J1746−2852, possibly SGR A East SNR
GEV J1800−2328.....	6.45, −0.19	22.5,12.0 (30.9)	5.4	6.3 ± 1.3	130 ± 27	2EG J1801−2312, possibly W28 SNR
GEV J1809−2327.....	7.47, −1.95	13.0	6.2	5.1 ± 1.0	105 ± 20	2EG J1811−2339
GEV J1732−1344.....	11.39, 10.56	25.6	5.0	2.4 ± 0.6	40 ± 10	2EG J1735−1312, QSO 1730−130
GEV J1814−1228.....	17.64, 2.32	24.7	5.0	4.6 ± 1.1	77 ± 18	2EG J1813−1229
GEV J1825−1310.....	18.25, −0.29	19.3	6.9	9.9 ± 1.7	169 ± 29	2EG J1825−1307
GEV J1837−0610.....	25.82, 0.33	12.0	6.0	8.3 ± 1.6	118 ± 23	...
GEV J1856+0115.....	34.58, −0.48	12.8	6.4	10.1 ± 1.9	108 ± 20	2EG J1857+0118, possibly W44 SNR
GEV J1907+0557.....	40.08, −0.88	22.9, 16.5 (22.8)	5.9	9.2 ± 1.9	85 ± 18	...
GEV J1613+3432.....	55.63, 46.39	48.7	5.0	2.3 ± 0.8	10 ± 4	2EG J1614+3431, QSO 1611+343
GEV J1636+3812.....	61.21, 42.15	29.9	8.1	4.8 ± 1.1	26 ± 6	2EG J1635+3813, QSO 1633+382
GEV J2020+3658.....	75.29, 0.24	16.7, 12.8 (69.1)	10.0	11.2 ± 1.5	159 ± 21	2EG J2019+3719
GEV J2020+4023.....	78.11, 2.16	8.1	12.7	14.8 ± 1.6	208 ± 23	2EG J2020+4026, possibly γ Cygni SNR
GEV J2026+4124.....	79.56, 1.86	35.9, 23.4 (146.9)	5.5	6.8 ± 1.5	93 ± 20	...
GEV J2035+4214.....	81.22, 1.02	25.4, 17.3 (25.0)	6.6	8.1 ± 1.5	108 ± 20	...
GEV J2253+1622.....	86.13, −37.93	29.8	7.9	3.5 ± 0.8	27 ± 6	2EG J2253+1615, QSO 2251+158
GEV J1835+5921.....	88.78, 25.11	16.4	14.2	10.2 ± 1.4	71 ± 10	2EG J1835+5919
GEV J0008+7304.....	119.78, 10.46	25.6	7.9	5.8 ± 1.2	40 ± 8	2EG J0008+7307, possibly CTA 1 SNR
GEV J0241+6102.....	135.90, 0.99	19.0	7.7	6.9 ± 1.3	62 ± 12	2EG J0241+6119, possibly LSI 61 303
GEV J0223+4254.....	140.27, −16.85	35.1	6.2	2.8 ± 0.7	25 ± 7	2EG J0220+4228, QSO 0219+428
GEV J0719+7133.....	143.74, 27.85	33.0	6.0	1.9 ± 0.5	26 ± 7	2EG J0720+7126, QSO 0716+714
GEV J0237+1648.....	156.37, −39.07	26.7	7.8	5.5 ± 1.2	32 ± 7	2EG J0238+1657, QSO 0235+164
GEV J0956+5508.....	159.00, 47.93	34.2	5.6	1.4 ± 0.4	20 ± 6	2EG J0957+5515, QSO 0954+556
GEV J0433+2907.....	170.50, −12.58	20.7	7.3	3.3 ± 0.7	54 ± 11	2EG J0432+2910
GEV J1104+3809.....	179.95, 65.07	18.3	9.3	2.8 ± 0.6	35 ± 7	2EG J1104+3812, Mkn 421
GEV J0534+2159.....	184.54, −5.84	4.6	34.6	21.4 ± 1.2	465 ± 25	2EG J0534+2158, Crab
GEV J0617+2237.....	189.02, 3.08	11.8	12.0	6.3 ± 0.8	121 ± 15	2EG J0618+2234, possibly IC 443 SNR
GEV J0530+1340.....	191.18, −11.05	18.3	8.2	3.0 ± 0.5	64 ± 11	2EG J0531+1324, QSO 0528+134
GEV J0634+1746.....	195.14, 4.30	5.0, 2.2 (56.2)	73.1	74.3 ± 2.2	1282 ± 39	2EG J0633+1745, Geminga
GEV J1222+2837.....	197.95, 83.49	22.6, 14.6 (13.7)	6.5	1.9 ± 0.5	22 ± 6	2EGS J1222+2821, QSO 1219+285
GEV J1201+2906.....	199.84, 78.76	28.0, 17.5 (8.1)	6.0	1.9 ± 0.5	21 ± 6	2EG J1158+2906, QSO 1156+295
GEV J0633+0645.....	204.83, −0.96	25.1	5.1	2.7 ± 0.7	42 ± 11	Possibly Monoceros SNR
GEV J0540−4359.....	250.01, −30.84	39.5	5.7	2.3 ± 0.7	19 ± 6	2EG J0536−4338, QSO 0537−441
GEV J0835−4512.....	263.58, −2.81	2.8, 2.1 (136.2)	78.4	148.1 ± 3.9	1759 ± 47	2EG J0835−4513, Vela
GEV J0210−5053.....	275.94, −61.87	12.3	14.7	8.5 ± 1.2	67 ± 9	2EG J0210−5051, QSO 0208−512
GEV J1025−5809.....	284.62, −0.58	33.2, 16.8 (64.6)	7.9	9.5 ± 1.6	109 ± 18	2EG J1021−5835
GEV J1059−5218.....	286.10, 6.86	22.6	7.4	4.7 ± 1.0	50 ± 10	2EG J1059−5224, PSR B1055−52
GEV J1047−5840.....	287.42, 0.41	16.9	7.4	7.5 ± 1.4	83 ± 15	2EG J1049−5847
GEV J1231−1357.....	295.50, 48.63	29.2	5.6	1.7 ± 0.5	25 ± 7	2EG J1233−1407
GEV J1256−0546.....	305.09, 57.08	8.5	19.1	6.9 ± 0.7	126 ± 13	2EG J1256−0546, 3C 279
GEV J1417−6100.....	313.18, 0.14	28.4, 13.3 (55.8)	6.6	9.8 ± 1.8	100 ± 19	2EGS J1418−6049
GEV J1409−0741.....	334.36, 50.32	30.8	6.2	2.0 ± 0.6	22 ± 6	2EG J1409−0742, QSO 1406−076
GEV J1709−4430.....	343.07, −2.68	6.6	17.6	20.0 ± 1.7	278 ± 23	2EG J1710−4432, PSR B1706−44
GEV J1626−2955.....	348.85, 13.19	16.5	9.1	4.9 ± 0.8	74 ± 12	PKS 1622−297
GEV J1626−2502.....	352.52, 16.53	22.7	6.0	3.2 ± 0.7	47 ± 11	2EG J1626−2452, QSO 1622−253
GEV J1732−3130.....	356.36, 0.95	32.6, 18.1 (0.8)	5.4	6.3 ± 1.3	127 ± 27	...

[a] See text for an explanation of each column.

degrees) following the convention of the second EGRET catalog (Thompson et al. 1995). The σ of a source is the square root of the maximum likelihood test statistic (Mattox et al. 1996a). The flux values are the mean flux and flux error over the entire mission, while the column labeled "photons" refers to the total number of estimated photons from the source. The flux values are given in units of 10^{-8} cm^{-2} s^{-1}. The final column gives a likely identification and/or association with a source reported either in the second EGRET catalog (Thompson et al. 1995) or in its supplement (Thompson et al. 1996). The criteria for identification are discussed in the following section. Of the 57

TABLE 2

LOW-SIGNIFICANCE SOURCES[a]

Source Name	Galactic Coordinates	Positional Error	σ	Flux	Photons	Identification
GEV J2024−0812.....	36.12, −24.35	46.4	4.7	2.5 ± 0.8	16 ± 5	2EG J2023−0836, QSO 2022−077
GEV J1957+2859.....	65.99, −0.09	21.6	4.7	3.9 ± 1.0	51 ± 13	...
GEV J2053+5644.....	94.42, 7.72	32.6	4.5	3.0 ± 0.9	28 ± 9	...
GEV J0319+2407.....	161.13, −27.60	42.2	4.6	2.1 ± 0.7	18 ± 6	...
GEV J0615+4200.....	171.45, 11.61	38.9	4.5	1.8 ± 0.6	22 ± 7	...
GEV J0508+0540.....	195.32, −19.81	37.0	4.5	1.4 ± 0.4	23 ± 7	...

[a] See text for an explanation of each column.

TABLE 3

VERY LOW SIGNIFICANCE SOURCES ASSOCIATED WITH PREVIOUSLY IDENTIFIED GAMMA-RAY SOURCES[a]

Source Name	Galactic Coordinates	Positional Error	σ	Flux	Photons	Identification
GEV J1832−2128.....	11.74, −5.80	25.6	4.2	2.2 ± 0.6	40 ± 12	2EG J1834−2138
GEV J2227+6101.....	106.40, 2.85	32.4	4.1	3.9 ± 1.2	29 ± 9	2EG J2227+6122
GEV J0441−0044.....	197.52, −28.87	68.4	4.1	1.4 ± 0.5	15 ± 5	2EGS J0442−0033, QSO 0440−003
GEV J0543−7031.....	281.09, −31.08	47.1	4.0	1.1 ± 0.4	15 ± 6	LMC
GEV J2009−4827.....	350.82, −32.66	49.4	4.1	2.2 ± 0.8	14 ± 5	QSO 2005−489

[a] See text for an explanation of each column.

sources, 27 are identified with objects seen at other wavelengths. The remaining unidentified sources are discussed in § 5.

4. IDENTIFIED SOURCES

Five of the sources given in Table 1 may be associated definitely with known pulsars, as they were in the EGRET catalogs. In order to study the possibility advanced in § 1 that GeV positions would suffer little in comparison with positions determined by using all photons above 100 MeV, we have listed the angular offset of the positions determined from the 100 MeV database (phases 1 and 2) and the 1 GeV database developed here (phases 1–4) in Table 4. We note no significant systematic difference, either way, in the offsets.

One of the sources given in Table 3 (GEV J0543−7031) is identified with the Large Magellanic Cloud. For the remaining sources, possible identifications were sought by using the extragalactic database (NED) (regardless of their Galactic latitude), using selection criteria similar to that of the first EGRET catalog (Fichtel et al. 1994). An identification was deemed likely if there was a positional coincidence within the 95% likelihood contour with a blazar, a loose category of active galactic nuclei (AGNs) that includes BL Lacertae objects, core-dominated, flat-spectrum radio quasars, and highly polarized and optically violently variable quasars.

Twenty-one of the sources were identified through the NED search as blazars, as is indicated in Tables 1–3. All of these blazar identifications have been given previously either in the second EGRET catalog (Thompson et al. 1995), in its supplement (Thompson et al. 1996), in an IAU telegram (Mattox et al. 1996b) for PKS 1622−297, or in a paper discussing the evolution of the EGRET AGN (Chiang et al. 1995) for blazar QSO 2005−489. QSO 2005−489 was also reported in the first EGRET catalog (Fichtel et al. 1994) but not in the second EGRET catalog or in its supplement. As for the pulsars, we have compared the angular offsets of the blazar source positions determined by the 100 MeV and 1 GeV studies. We do not have the positional information for one EGRET blazar source, PKS 1622−297; however, for the 20 remaining blazars, we have made the comparison. In Figure 4 histograms of the angular offsets for these 20 blazars are shown. The average offset for positions from the EGRET catalog positions is 0°.31; for the GeV catalog positions, an average offset of

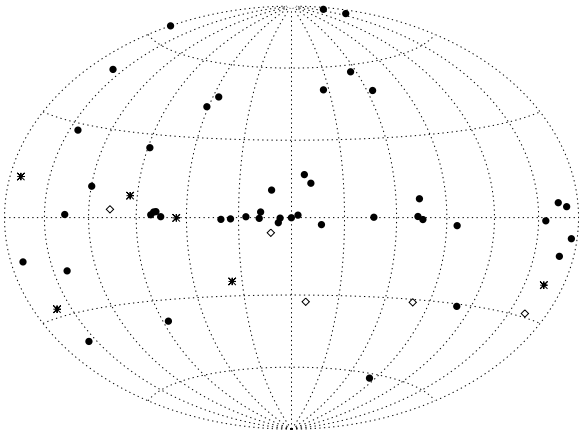

FIG. 3.—Locations of the 57 sources given in Tables 1–3. The filled circles correspond to the high-significance sources of Table 1; the stars correspond to the low-significance sources of Table 2; the diamonds correspond to previously seen sources with significances between 4.0 and 4.5 σ.

TABLE 4

COMPARISON OF PULSAR POSITIONS

Source Name	GeV Catalog Angular Offset (deg)	EGRET Catalog Angular Offset (deg)
Vela pulsar	0.04	0.04
Geminga pulsar.....	0.04	0.02
Crab pulsar	0.06	0.07
PSR B1706−44.....	0.03	0.27
PSR B1055−52.....	0.23	0.08

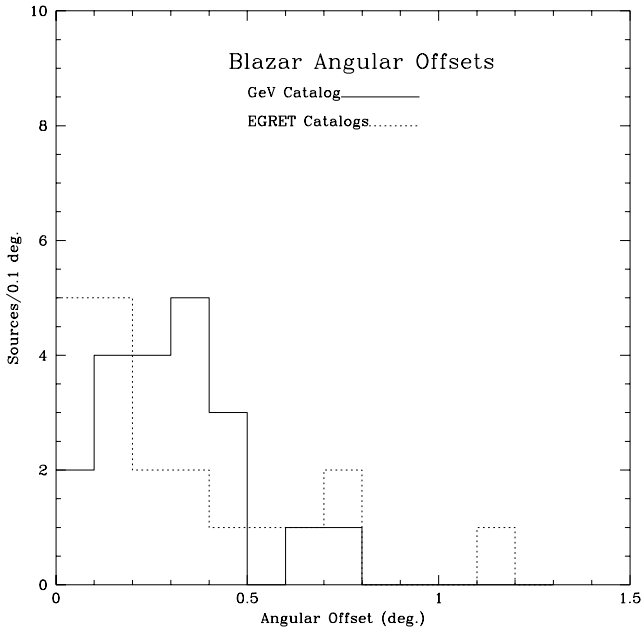

FIG. 4.—Histograms of the angular offsets for the 20 blazar identifications common to the EGRET and GeV catalogs. The average offset for each of the two catalogs is the same, 0°.31.

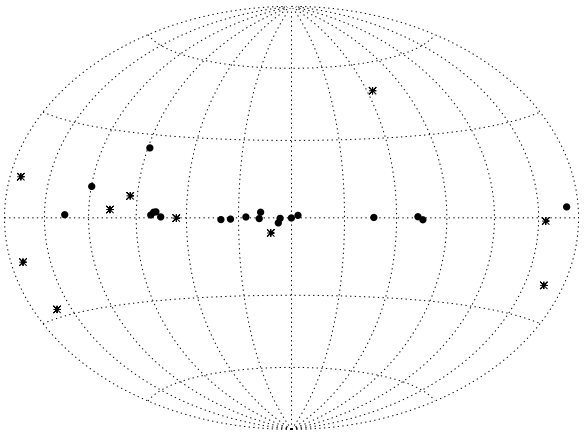

FIG. 5.—Locations of the 30 unidentified sources

0°.31 is also obtained. Thus, in spite of the substantial loss in photon statistics, there is little or no degradation of the positional accuracy caused by the restriction to GeV energy photons.

5. UNIDENTIFIED SOURCES

In the combined list of sources in Tables 1–3, 30 sources have no firm identification (other than possibly an identification with an EGRET catalog source). Identification with an otherwise unidentified 100 MeV source is based on having the 95% confidence contours for the two positions overlap. In Figure 5 the positions of these sources are plotted; they show an obvious clustering about the Galactic equator, with only one source having a Galactic latitude greater than 30°.

In order to make a quantitative test of how uniform this distribution is, one must make corrections for both the nonuniform background and the nonuniform exposure. If the γ-ray sources are distributed uniformly in Euclidean space, the number of sources N above a given minimum flux $F_{\rm min}$ will be proportional to $F_{\rm min}^{-3/2}$. Mattox et al. (1996a) have shown that at a given threshold of statistical significance, $F_{\rm min}$ will vary as $(B/E)^{1/2}$, where B is the background intensity (independent of exposure) and E is the total exposure. Thus, if background variations can be neglected, N will scale as $E^{3/4}$.

On the basis of the EGRET exposure (Fig. 2), if the 30 unidentified sources are distributed uniformly and we neglect the growth of the background as one moves toward the Galactic equator, one would expect approximately 12 sources to have a Galactic latitude greater than 30°, whereas only one is seen. Furthermore, if the diminished sensitivity to sources resulting from increased background toward the plane is taken into account, the conclusion that the distribution is Galactic is even stronger.

In an effort to categorize these sources further, one-dimensional projections of their longitude and latitude values are plotted in Figures 6*a* and 6*b*. The dashed curves in Figure 6 give the EGRET exposure to the U power, normalized to having the same area as the histograms.

The longitude distribution of Figure 6*a* shows no strong contrast between directions toward or away from the Galactic center. For example, in the interval $-30°$ to $+30°$ toward the Galactic center, there are eight sources, whereas in the anticenter region from -150 to $+150$, there are six sources. If these sources were at distances of more than the typical separation distance between spiral arms of the Galaxy (2–3 kpc), they would be expected to show a significant enhancement in the regions toward the center. From the general lack of strong contrast, one may conclude that these sources are generally at distances of less than ~ 5 kpc. Studies of the longitude distribution of the unidentified sources in the 100 MeV catalogs (Mukherjee et al. 1995; Kanbach et al. 1996) reach a similar conclusion.

The latitude distribution of the sources (Fig. 6*b*) shows a clustering about $b = 0°$, with wings that extend to beyond 20°. This distribution is not consistent with a simple Gaussian distribution. A two-dimensional scatter plot of source flux versus Galactic latitude (shown in Fig. 7) suggests a

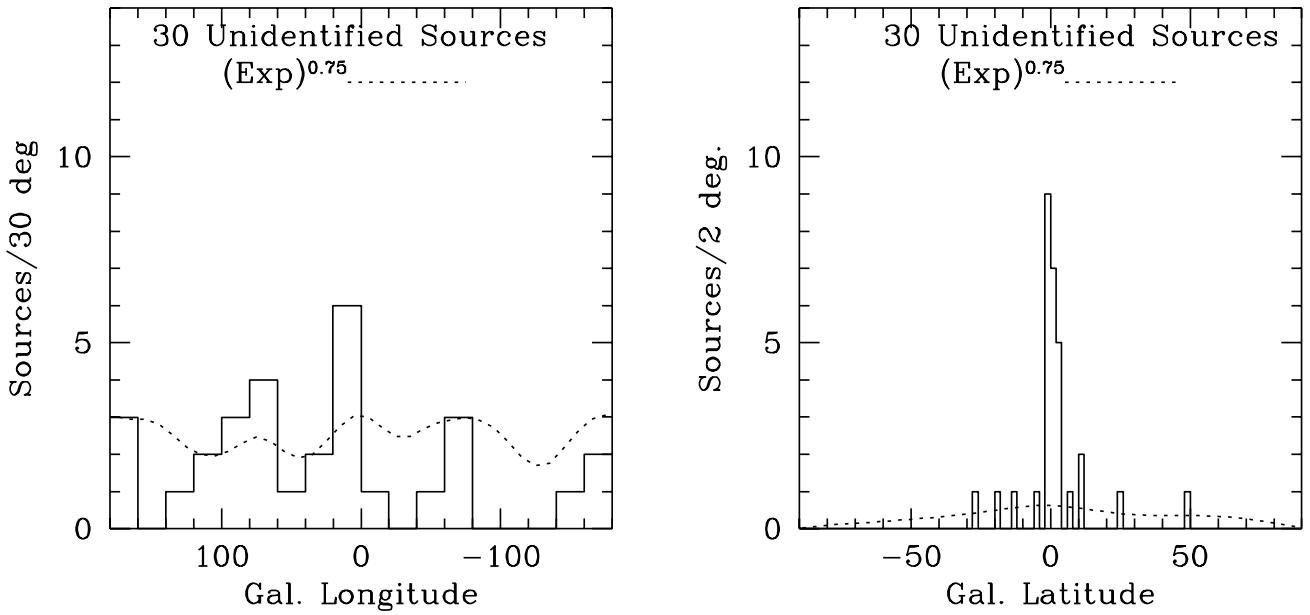

FIG. 6.—(*a*) Galactic longitude and (*b*) Galactic latitude distributions of the 30 unidentified sources. The total exposure, raised to the U power and normalized to have the same area as the histograms, is shown as dotted lines in each plot.

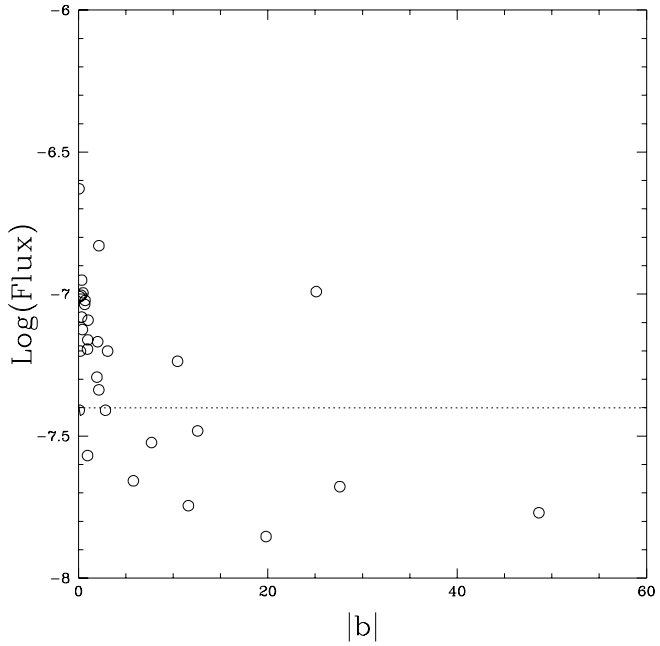

FIG. 7.—Flux vs. b scatter plot for the 30 unidentified sources. The dashed line indicates the flux value that separates "bright" from "dim" sources.

distinction between two types of source. One category ("bright") has a clustering near the Galactic equator. The other category ("dim") has a much broader distribution in latitude. The separation between these two categories can be made empirically at a flux value of 4×10^{-8} photons cm^{-2} s^{-1}. With this demarcation, 20 sources are bright, and 10 are dim. The bright sources have an average $b = 2.^{\circ}7$, whereas the average b for the dim sources is $13.^{\circ}8$. We note that of the 10 so-called new sources, i.e., sources that have not previously been reported in the second EGRET catalog (Thompson et al. 1995) or in its supplement (Thompson et al. 1996), five are in the bright category and five are in the dim category.

The absence of high-latitude bright sources is striking. For example, although there are twice as many bright sources (20) as dim (10), only two bright sources occur at latitudes greater than 5°, whereas there are seven dim sources. This feature is consistent with the fact that the bright sources are strongly clustered along the Galactic plane. The lack of dim sources at latitudes less than 5° may be caused by a diminished sensitivity near the plane from the increasingly diffuse background and from possible confusion resulting from brighter pointlike sources. Note that one of the dim sources in the anticenter region, GEV J0633+0645, may possibly be identified with the Monoceros supernova remnant (SNR), as listed in Table 4.

The average luminosity of the bright sources may be constrained by a line of reasoning similar to that of Mukherjee et al. (1995) for the unidentified Galactic plane sources given in the first EGRET catalog (Fichtel et al. 1994). If we take a minimum scale height of 40 pc, then the average latitude of the bright GeV sources of $2.^{\circ}7$ translates into a minimum average distance of ~ 1 kpc. This corresponds to a luminosity (1–10 GeV) of $\sim 4 \times 10^{34}$ ergs s^{-1} for a source with a flux of 1×10^{-7} photons cm^{-2} s^{-1}. With a scale height of ~ 100 pc, common to many Population I objects, an average luminosity of $\sim 3 \times 10^{35}$ ergs s^{-1} (1–10 GeV) results. This luminosity is in rough agreement with the estimates given by Mukherjee et al. (1995) and by Kanbach et al. (1996).

Previous authors (Sturner, Dermer, & Mattox 1996; Esposito et al. 1996) have suggested that several of the low-latitude bright sources may be associated with radio SNRs. Table 5 lists these likely associations. In this table we have included one of the dim sources, GEV J0633+0645. The possibility that CTA 1 is a counterpart of a previously unidentified γ-ray source has typically been overlooked by studies that focused on SNRs within 10° of the Galactic plane. (X-ray observations of CTA 1 by Seward, Schmidt, & Slane 1995 reveal a coincident $z = 0.225$ AGN. This AGN is therefore, an alternative possible identification for the γ-ray source GEV J0008+7304 at this position.) Distances to these SNRs are those given in Esposito et al. (1996) with the exception of CTA 1, taken from Pineault et al. (1993). Note that the distances are fully consistent with the upper limit of 5 kpc given above. The nature of the remaining 14 bright sources remains a mystery. Perhaps several of them may be previously undetected SNRs. Another possibility is that some are previously undetected, fast, young radio pulsars, as was recently discussed by Kaaret & Cottam (1996) and Yadigaroglu & Romani (1997). Kaspi (1997) has supplied a specific example of a likely association of a low-latitude, EGRET unidentified source with a young, fast (63 ms period) radio pulsar that she has discovered. Brazier et al. (1996) have proposed that the source 2EG J2020+4026 (GEV J2020+4023) may be a young pulsar.

We now consider the dim unidentified sources. Figure 8 gives the cumulative distribution (normalized to 1) of the absolute Galactic latitude of these sources in comparison with the cumulative distribution of the U power of the exposure. The maximum deviation of the data is 0.44. The application of the Kolmogorov-Smirnov test to this statistic allows the hypothesis that the dim sources are consistent with an isotropic distribution to be rejected at greater than the 97% confidence level. This conclusion is further strengthened when the increased background near the Galactic equator is taken into account, since it works to diminish the number of dim sources that are detected near the plane.

From their average Galactic latitude, a minimum average distance of ~ 200 pc may be derived for the dim sources. Their maximum distance is not well constrained, since they could be as far as 5 kpc, on the basis of their longitude distribution, in which case they would have a scale height of ~ 1 kpc.

If the dim sources have the same scale height as the bright sources, then an average luminosity of ~ 2 orders of magnitude less than the bright sources results. If one assumes an

TABLE 5

UNIDENTIFIED GeV SOURCES WITH POSSIBLE SNR ASSOCIATIONS

GeV Source Name	SNR	Radio Flux	Estimated Distance (kpc)
GEV J1800−2328.....	W28	310	1.8–4.0
GEV J1856+0112.....	W44	230	3
GEV J2020+4023.....	γ Cygni	340	1.8 ± 0.6
GEV J0617+2237.....	IC 443	160	0.7–2.0
GEV J0633+0645.....	Monoceros	160	0.8–1.6
GEV J1746−2854.....	Sgr A East	100	...
GEV J0008+7304.....	CTA 1	36	1.7 ± 0.3

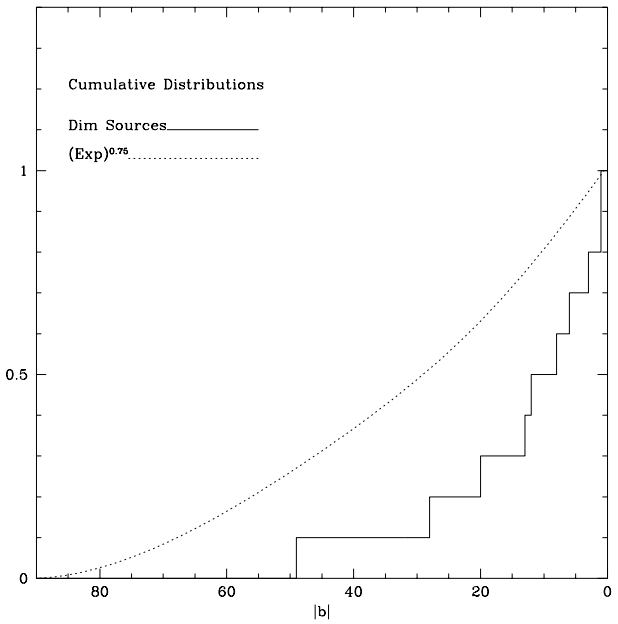

FIG. 8.—Cumulative distribution of the Galactic latitude of the dim, unidentified sources, compared to the cumulative distribution of the total exposure to the U power.

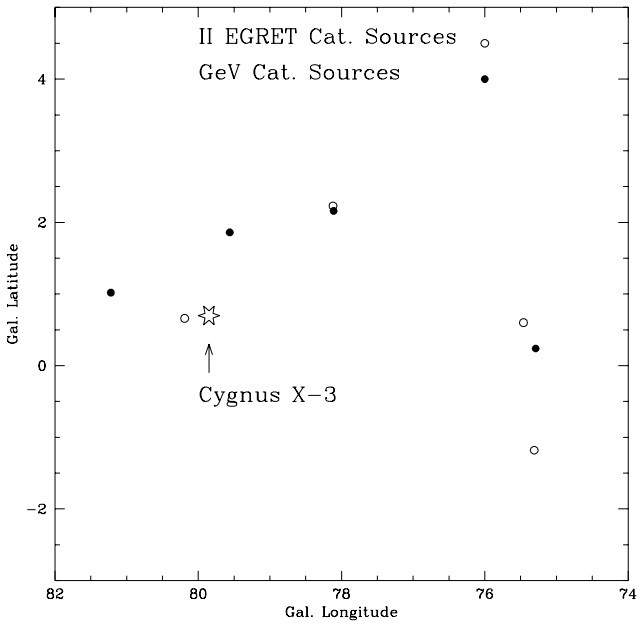

FIG. 9.—Sources located in the Cygnus region

average distance of 500 pc for the dim sources (appropriate to a 100 pc scale height), then an average luminosity of $\sim 3 \times 10^{33}$ ergs s^{-1} (1–10 GeV) results. What are some of the possibilities for their identification? One is that they are Geminga-like pulsars, i.e., pulsars that shine brightly in γ-rays but are relatively dim at other wavelengths. Although the scale height of Geminga-like pulsars is not well constrained, the average luminosity for the dim unidentified objects could be consistent with this possibility. This possibility has been advanced most recently in the study of unidentified EGRET sources by Mukherjee et al. (1995). They conclude that the $b > 10°$ unidentified EGRET sources could be Geminga-like pulsars. Other possibilities for the high-latitude, unidentified EGRET sources are given by Özel & Thompson (1996), and these same possibilities would hold for the unidentified sources discussed here.

5.1. *Cygnus Region Complex*

In the second EGRET catalog, four sources are located within approximately 5° of each other near Galactic latitude 80°. One of these sources may possibly be identified with Cygnus X-3 (Mori et al. 1997). However, the analysis of the region is very difficult, since it is a region of enhanced diffuse emission (Hunter et al. 1997) and the PSF of the EGRET instrument will simultaneously overlap the positions of all four of the EGRET sources. One of the motivations for this work was the thought that by using only the higher energy EGRET photons, source confusion would be minimized.

Figure 9 shows the locations of the GeV catalog sources as well as the EGRET sources. Note that for two of the sources, there is essential agreement in the positions reported. However, there is no positional identification of a GeV source with Cygnus X-3. If Cyg X-3 is a steady γ-ray source, its flux (>100 MeV) of $8.2 \pm 0.8 \times 10^{-7}$ cm^{-2} s^{-1} and relatively hard spectral index of 1.9 (Mori et al. 1997) would indicate that there should be a significantly detectable flux above 1 GeV. The lack of such a detection indicates that the spectrum breaks in the sub-GeV range. One of the four sources in the Cygnus region (GEV J2020+4023) is possibly associated with SNR γ Cygni (as noted in Table 4).

6. CONCLUSIONS

In the GeV γ-ray catalog presented here, we have reported 10 sources not previously cataloged. Blazar identifications previously given in the EGRET catalogs are supported. However, the GeV γ-ray sky is somewhat different from the sky as seen by the previous EGRET catalogs. Most, if not all, of the unidentified GeV sources are Galactic. Furthermore, there appears to be a possible separation of the unidentified sources into two categories, based on relative brightness. One category, composed of brighter sources, has a Galactic latitude distribution consistent with that of the radio SNRs. The other source category, dim and near the sensitivity limit of EGRET, could be consistent with a relatively nearby (200–1000 pc) distribution of Geminga-like pulsars and would be 2 orders of magnitude less luminous, on average, than the bright sources. Other possibilities exist, however.

A major problem that has confronted high-energy γ-ray astronomy since the days of the *SAS-2* and *COS-B* satellites is the issue of source identification. It is hoped that this catalog may stimulate further progress in this critical area and that it may also be used to guide efforts by ground-based γ-ray observatories in their search for sources of even higher energy photons.

We acknowledge useful conversations with Stewart Anderson, David Bertsch, Marshall Cohen, Chuck Dermer, John Mattox, Pat Nolan, Tom Prince, David Thompson, and Dan Williams. This research has been supported in part by NASA guest investigator grants for the *Compton Gamma Ray Observatory*. This research has made use of the NASA/IPAC Extragalactic Database (NED), which is operated by the Jet Propulsion Laboratory, California Institute of Technology, under contract with NASA.

REFERENCES

Bertsch, D. L., et al. 1993, ApJ, 416, 587
Brazier, K. T. S., Kanbach, G., Carramiñana, A., Guichard, J., & Merck, M. 1996, MNRAS, 281, 1033
Chiang, J., Fichtel, C. E., von Montigny, C., Nolan, P. L., & Petrosian, V. 1995, ApJ, 452, 156
Dingus, B. L., et al. 1996, ApJ, 467, 589
Esposito, J. A., Hunter, S. D., Kanbach, G., & Sreekumar, P. 1996, ApJ, 461, 820
Fichtel, C. E., et al. 1994, ApJS, 94, 551
Hunter, S. D., et al. 1997, ApJ, 481, 205
Kaaret, P., & Cottam, J. 1996, ApJ, 462, L35
Kanbach, G., et al. 1988, Space Sci. Rev., 49, 69
———. 1996, A&AS, 120, 461
Kaspi, V. M. 1997, in Proc. Fourth Compton Symp., ed. C. D. Dermer, J. D. Kurfess, & M. S. Strickman (New York: AIP)
Lin, Y. C., et al. 1996, ApJS, 104, 331
Mattox, J. R., et al. 1996a, ApJ, 461, 369
Mattox, J. R., Wagner, S., McGlynn, T. A., Malkan, M., & Schachter, J. F. 1996b, IAU Circs. 6179, 6181
Mori, M., et al. 1997, ApJ, 476, 842
Mukherjee R., Bertsch, D. L., Dingus, B. L., Kanbach, G., Kniffen, D. A., Sreekumar, P., & Thompson, D. J. 1995, ApJ, 441, L61
Nolan, P. L., et al. 1996, ApJ, 459, 100
Ong, R., et al. 1996, in Padua Workshop on TeV Gamma-Ray Astrophysics, ed. M. Cresti (Padua: Univ. Padua Press), 261
Özel, M., & Thompson, D. J. 1996, ApJ, 463, 1050
Pineault, S., Landecker, T. L., Madore, B., & Gaumont-Guay, S. 1993, AJ, 105, 1060
Québert, J., et al. 1996, Padua Workshop on TeV Gamma-Ray Astrophysics, ed. M. Cresti (Padua: Univ. Padua Press), 248
Seward, F. D., Schmidt, B., & Slane, P. 1995, ApJ, 453, 284
Sreekumar, P., et al. 1996, ApJ, 464, 628
Sturner, S. J., Dermer, C. D., & Mattox, J. R. 1996, A&AS, 120, 445
Thompson, D. J., et al. 1993, ApJS, 86, 629
———. 1995, ApJS, 101, 259
———. 1996, ApJS, 107, 227
Yadigaroglu, I.-A., & Romani, R. W. 1997, ApJ, 476, 347
Weekes, T. C. 1996, in Proc. Texas Symp. on Relativistic Astrophysics, ed. A. Olinto, J. Frieman, & D. Schramm (Singapore: World Scientific)